Accelerated Neonatal fMRI using Multiband EPI

Anthony N. Price[1,2], Lucilio Cordero-Grande[1,2], Shaihan J. Malik[1,2], Maryam Abaei[1], Tomoki Arichi[1], Emer J. Hughes[1], Daniel Rueckert[3], A. David Edwards[1], and Joseph V. Hajnal[1,2]

[1]*Centre for the Developing Brain, King's College London, London, United Kingdom,* [2]*Division of Imaging Sciences & Biomedical Engineering, King's College London, London, United Kingdom,* [3]*Biomedical Image Analysis Group, Imperial College London, London, United Kingdom*

Target Audience: Researchers interested in utilising multiband capability for fMRI and its application to neonatal subjects

Purpose: Multi-Band (MB) imaging can be used to accelerate functional MRI based on 2D GE-EPI, increasing the sampling rate and improving detection of resting state networks (RSN) [1,2]. The ability to sample faster than patient cardiac and respiratory physiology allows separation of signals correlated with these sources and the signals of interest related to spontaneous brain activity. However, applying this in the neonatal population places even higher demands, due to their naturally high respiratory and heart rates. Here we present preliminary results of using MB to accelerate GE-EPI fMRI to sampling rates sufficient to resolve neonatal cardiac physiology and provide increased RSN detection compared to standard neonatal fMRI protocol.

Methods: MB radio frequency (RF) pulses (Figure 1) were generated offline (Matlab, MathWorks) with a predefined slice thickness and gap, Bloch simulations were used to check profile fidelity and to adjust outer slice amplitudes to compensate for attenuation due to the dwell time of the RF waveform generator. MB pulses with amplitude but no phase modulation were found to produce the purest slice profiles. To minimise peak B_1, optimal phase offsets were found which gave purely real waveforms; reductions in peak B_1 achieved for MB9 was 4.55 x the single-band (SB) peak B_1. Pre-distortion of RF pulses was necessary to account for the non-linear response of the RF amplifier. A linearly incrementing shift pattern of FoV/3 was used to shift adjacent MB slices. A SB acquisition with matched EPI readout bandwidth was also collected for coil sensitivity reference data.

1

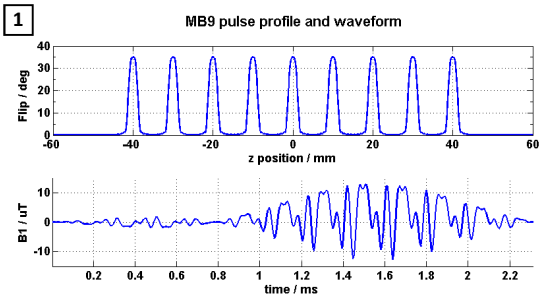

Data were collected on a Philips 3T Achieva system using a dedicated neonatal head coil with 32 receive elements (RAPID GmbH, Rimpar DE). Two preterm infants (gestational ages: 28, 32 weeks, both scanned at 34 weeks post-menstrual age, body mass: 1770,1620g) were scanned unsedated with routine monitoring throughout, according to local ethics, and under parental consent. A peripheral pulse unit (ppu) and pressure bellows (resp) was used to collect cardiac and respiratory physiology data during image acquisition; this was analysed to produce a power spectral density (PSD) plot. An established standard single-band (SB) fMRI protocol for neonatal resting state fMRI [3] was used as a comparison to MB9 accelerated data sets. Both protocols were 2.5x2.5mm in-plane acquired resolution; SB employed 3.25mm slices + 0.75mm gap, whereas MB9 was enhanced to 2.5mm contiguous slices. Each protocol was ran for 5 minutes leading to a total number of dynamics and (TR per volume) of SB = 200/(1.5s); and MB9 = 920/(0.32s).

Images were reconstructed offline utilising ReconFrame (GyroTools, Zurich) and custom unfolding scripts written in Matlab. Reconstruction of multiband images is formulated as a linear inverse problem considering the coil sensitivities, the multiband encoding pattern and the EPI ghost correction terms. Reconstructed image and ghosting parameters are estimated from the measured data in an alternating fashion by using, respectively, the conjugate gradient algorithm [4] and the Newton method. Standard fMRI data pre-processing was applied included brain extraction, motion correction, and spatial smoothing (FWHM 3mm). For each run, ICA components were estimated with MELODIC (Beckmann and Smith, 2005) and the power spectrum of the BOLD signal timeseries at a voxel within the identified visual RSN were calculated for SB and MB9 data.

Results and Discussion Figure 1 illustrates the MB9 pulse generated using phase conjugate symmetry to offset slice phases, resulting in AM only modulation. Bloch simulations show the desired flip angle has been achieved after RF sampling (6.4us) correction. Figure 2 shows the power spectrum of a section (~1 minute) of the ppu and resp traces recorded during one MB9 scan (same scan used in Fig. 3), showing the true cardiac frequency component at ~2.7Hz (162 bpm) and respiratory components ranging 0.5-1Hz. Re-sampling the ppu trace at the rate of the SB and MB9 acquisitions indicates the alias of the cardiac component for MB9 (0.3Hz) remains clear of the main low frequency oscillations (LFO) of interest. Figure 3b shows the power spectrum from the MB9 fMRI data for a voxel in the visual RSN after ICA decomposition. This demonstrates both respiratory and cardiac components. For the SB acquisition sampled at TR=1.5s (or 0.67Hz), respiratory and cardiac sources get aliased into the LFO range. Although MB9 in this case is sufficient to resolve cardiac components, the neonatal heart rate can fluctuate significantly, and so higher sampling would be advantageous. Current work focuses on determining whether higher MB accelerations can produce data of sufficient quality across the whole brain, particularly as additional increases in spatial resolution are also desired if adequate signal-to-noise and temporal acceleration can be achieved.

2

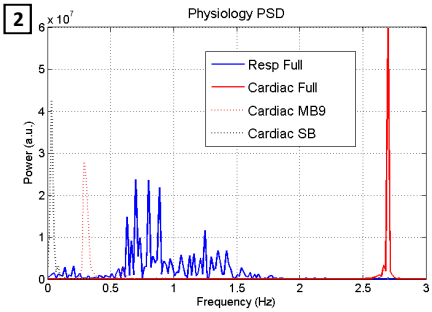

3a

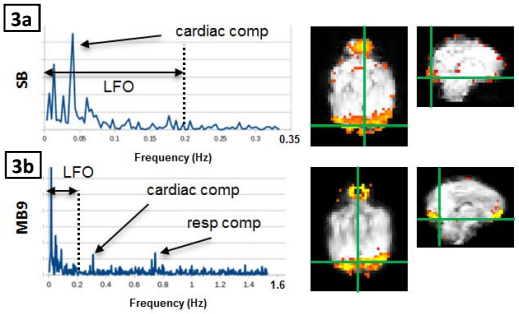

Conclusions Highly accelerated fMRI has been demonstrated in the neonatal brain using multiband acquisitions sufficiently fast to differentiate the rapid cardiac components of even preterm infants. Detection of additional components has been observed compared to traditional single-band fMRI acquisition which should lead to improved detection of resting state networks.

References: [1] Setsompop et al. 2012: MRM 67:1210-1224. [2] Feinberg et al. Journal of Magnetic Resonance 229 (2013) 90–100. [3] Arichi, T et al., NeuroImage, 49(3)2010:2063-71 [4] Pruessmann, K.P., Weiger, M., et al., Magn. Reson. Med., 46:638-51; 2001.

Acknowledgments: Many thanks to Martin Buehrer (GyroTools) and Steen Moeller (CMRR) for valuable advice; MRC strategic funds, GSTT BRC, and the ERC for dHCP project funding.